iScience

Article

Spatiotemporal proteomic and transcriptomic landscape of DAT+ dopaminergic neurons development and function

Graphical abstract

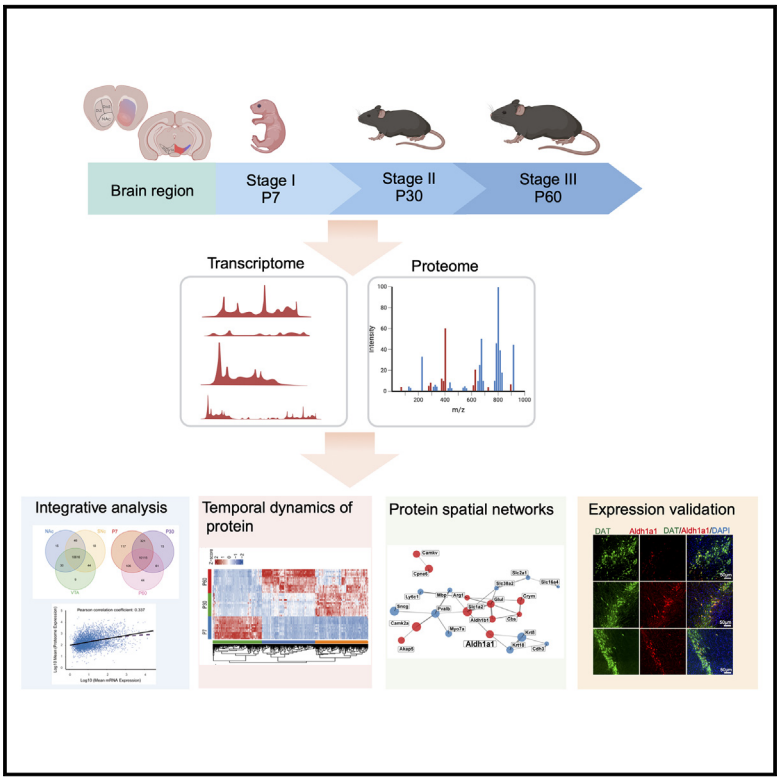

Authors

Heyu Zhao, Peipei Chen, Xia Gao, Zhili Huang, Pengyuan Yang, Huali Shen

Correspondence

shenhuali@fudan.edu.cn

In brief

Molecular biology; Neuroscience; Omics

Highlights

- Utilized trace proteomics and SMART-seq2 to characterize DAT+ neuron development
- Profiled DAT^{+} neurons across brain regions (NAc, SNc, and VTA) and stages (P7, P30, and P60)
- Identified Aldh1a1's dynamic role in DA neuron maturation
- Revealed distinct molecular signatures reflecting DAT+ neuron functional diversity

Zhao et al., 2025, iScience *28*, 112115
April 18, 2025
https://doi.org/10.1016/j.isci.2025.112115

CellPress

iScience

CellPress
OPEN ACCESS

Article

Spatiotemporal proteomic and transcriptomic landscape of DAT+ dopaminergic neurons development and function

Heyu Zhao,[1,3] Peipei Chen,[1,2,3] Xia Gao,[1] Zhili Huang,[2] Pengyuan Yang,[1,4] and Huali Shen[1,5,*]
[1]Institutes of Biomedical Sciences, Fudan University, Shanghai 200032, China
[2]Department of Pharmacology, School of Basic Medical Sciences, Fudan University, Shanghai 200032, P.R. China
[3]These authors contributed equally
[4]Deceased
[5]Lead contact
*Correspondence: shenhuali@fudan.edu.cn
https://doi.org/10.1016/j.isci.2025.112115

SUMMARY

Dopaminergic (DA) neurons expressing the dopamine transporter (DAT) play vital roles in physiology and the regulation of mental and neurological disorders. This study investigates spatiotemporal proteomic and transcriptomic changes in DAT+ DA neurons from key brain regions—the nucleus accumbens (NAc), substantia nigra (SNc), and ventral tegmental area (VTA)—at postnatal milestones: day 7 (P7), day 30 (P30), and day 60 (P60). Using advanced multi-omics techniques, including ultrasensitive trace sample proteomics and SMART-seq2, we reveal distinct molecular profiles within DA neuron populations, reflecting their developmental progression and functional roles. Immunofluorescence mapping validates these findings and underscores the dynamic molecular architecture of DA neurons. *Aldh1a1* expression, a key enzyme for retinoic acid production, progressively increases over time, reflecting its involvement in neuronal development and specialized functions. This study provides valuable insights into the development and function of DAT+ DA neurons.

INTRODUCTION

The majority of midbrain dopaminergic (mDA) neurons, the primary source of dopamine in the central nervous system (CNS), are localized within three nuclei: the substantia nigra pars compacta (SNc), the ventral tegmental area (VTA), and the retrorubral field (RRF).[1] DA neurons in the SNc regulate the dorsal striatum via the nigrostriatal pathway, while VTA neurons project to the NAc, olfactory tubercle, and prefrontal cortex, forming the mesolimbic and mesocortical systems.[2] These neurons coordinate various physiological and behavioral processes, including movement, sleep, learning, memory, emotions, and motivated behaviors. They are also implicated in neuropsychiatric disorders such as Parkinson's disease, depression, and addiction.[3–5]

Recent single-cell studies focusing on the embryonic development of mDA neurons have characterized their functional heterogeneity and molecular diversity.[6,7] However, our understanding of the molecular diversity in the later stages of DA neuron development, particularly in terms of axonal growth and synaptic connections, remains limited. Meanwhile, mass spectrometry-based proteomics have provided insights into the molecular characteristics of VTA and SNc neurons,[8,9] but further research is necessary to elucidate the complexities of their later developmental stages.

Midbrain ventral DA neuron development involves regional specification, induction, differentiation, post-mitotic development, migration, and axonal growth.[10,11] Proteins essential for developmental functions continue to be expressed in post-mitotic neurons throughout life, transitioning from developmental roles to those involved in survival and maintenance. For instance, proteins such as *Nurr1* and *Pitx3*, which are crucial during early development, are also involved in the long-term maintenance of DA neurons.[12,13] While embryonic development has been extensively studied, reports on the postnatal development of these neurons are scarce. Identifying previously uncharacterized proteins offers mechanistic insights into diverse developmental stages and sheds light on their susceptibility to and degeneration in neuropsychiatric disorders, such as Parkinson's disease. This ongoing expression and functional shift highlight the importance of postnatal studies in understanding DA neuron biology and pathology.

Sparse labeling and functional methods have defined subsets of mDA neurons.[14,15] For instance, VTA projections to the NAc core, but not the medial shell, are involved in acquiring motivational value for rewards, while aversion-coding VTA neurons project to the medial shell but not the core.[16] Despite extensive studies on VTA-to-NAc projections, their heterogeneity has complicated the assignment of specific functions to molecular subtypes.

In this study, we delve into the multi-omics landscape of DAT+ neurons across three postnatal developmental stages. Employing

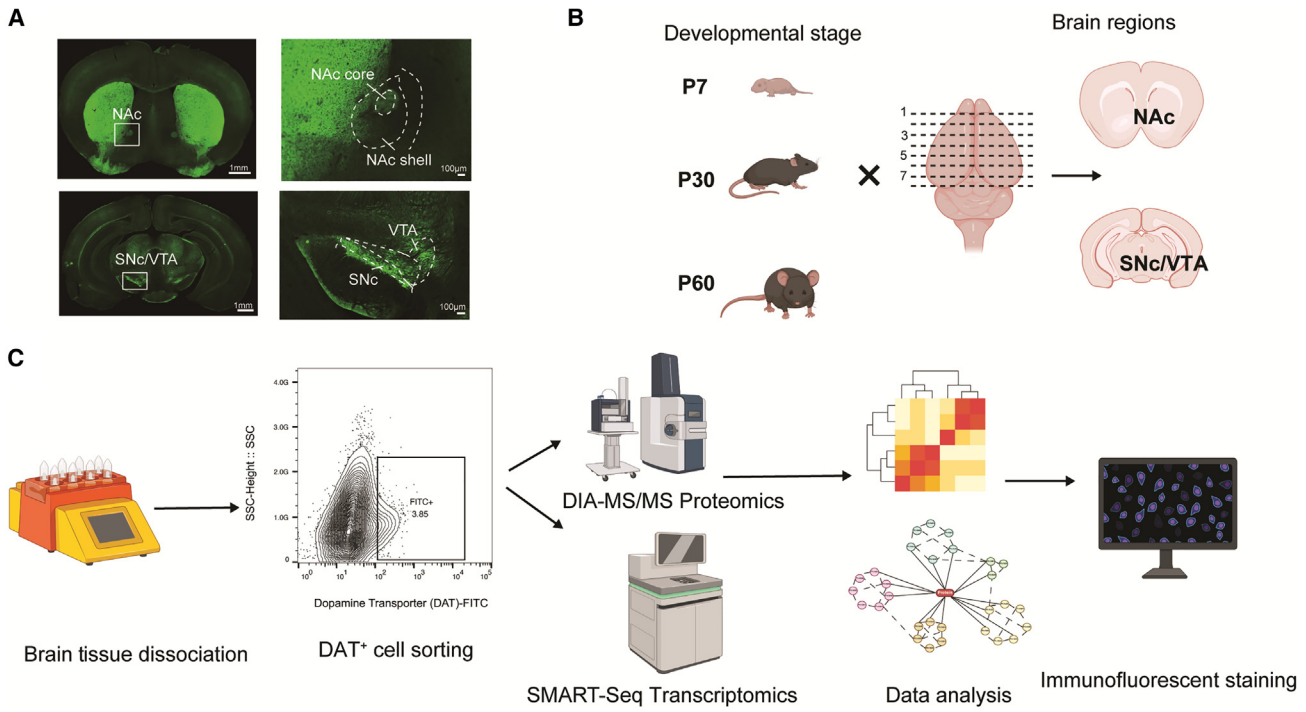

Figure 1. Spatiotemporal proteomic and transcriptomic profiling of DAT+ dopaminergic neurons in the mouse brain

(A) Fluorescence imaging of DAT+ neurons within the NAc region (top left) and across the SNc/VTA regions (bottom left), with magnified views of the NAc core and shell, and the SNc and VTA (right panels), showing spatial distribution.

(B) Schematic representation of the experimental design, including brain dissection of the NAc, SNc, and VTA regions at developmental stages P7, P30, and P60.

(C) Workflow illustrating brain tissue dissociation, followed by fluorescence-activated cell sorting (FACS) for DAT+ neurons, with the FACS scatterplot showing the gating strategy and percentage of isolated FITC$^+$ cells. Subsequent multi-omics analyses (DIA-MS/MS proteomics and SMART-seq2 transcriptomics) are shown along with data analysis steps (e.g., heatmap and network analysis) and immunofluorescent validation of molecular markers.

ultrasensitive trace sample proteomics developed in our laboratory[17] and SMART-seq2 for transcriptomics,[18] we meticulously analyzed small yet distinct regions in mouse brain, including NAc, SNc, and VTA. By building extensive datasets of DAT+ neurons from NAc, SNc, and VTA of the mouse brain at P7, P30, and P60, we illuminate the complex spatiotemporal dynamics and molecular diversity of DA neurons throughout postnatal development. Understanding the development and function of DA neurons is crucial for elucidating the mechanisms underlying various neurological and psychiatric disorders, and this refined knowledge has significant implications for advancing basic neuroscience research and uncovering fundamental principles of brain function.

RESULTS

In this study, we employed a comprehensive multi-omics approach to profile the development of DAT+ neurons across various developmental stages and brain regions. Our analysis encompassed proteomic and transcriptomic techniques to unravel the complex molecular landscape and interactions within these neurons. Here, we present our findings in a stepwise manner, beginning with an overview of the experimental workflow, followed by detailed results on gene expression profiles, identification of molecular contributors, and validation experiments of our datasets.

Comprehensive workflow for profiling DAT+ dopaminergic neurons in mouse brain

We employed a multi-omics approach to explore the molecular development of DAT+ neurons across key brain regions and developmental stages in mice. This integrated strategy, combining proteomic and transcriptomic profiling, provided a detailed understanding of the complex molecular changes associated with dopaminergic neuron maturation.

To capture these developmental insights, we selected mice at three distinct stages—P7 (infancy), P30 (juvenile), and P60 (adult)—with five biological replicates per group. Our focus was on three specific brain regions known for their high density of DAT+ neurons: the nucleus accumbens (NAc), substantia nigra pars compacta (SNc), and ventral tegmental area (VTA). Fluorescence imaging highlighted the spatial distribution of DAT+ neurons within these regions, offering a visual confirmation of their localization (Figures 1A and 1B).

After isolating the target brain regions, tissue samples were dissociated into single-cell suspensions. FACS was then utilized

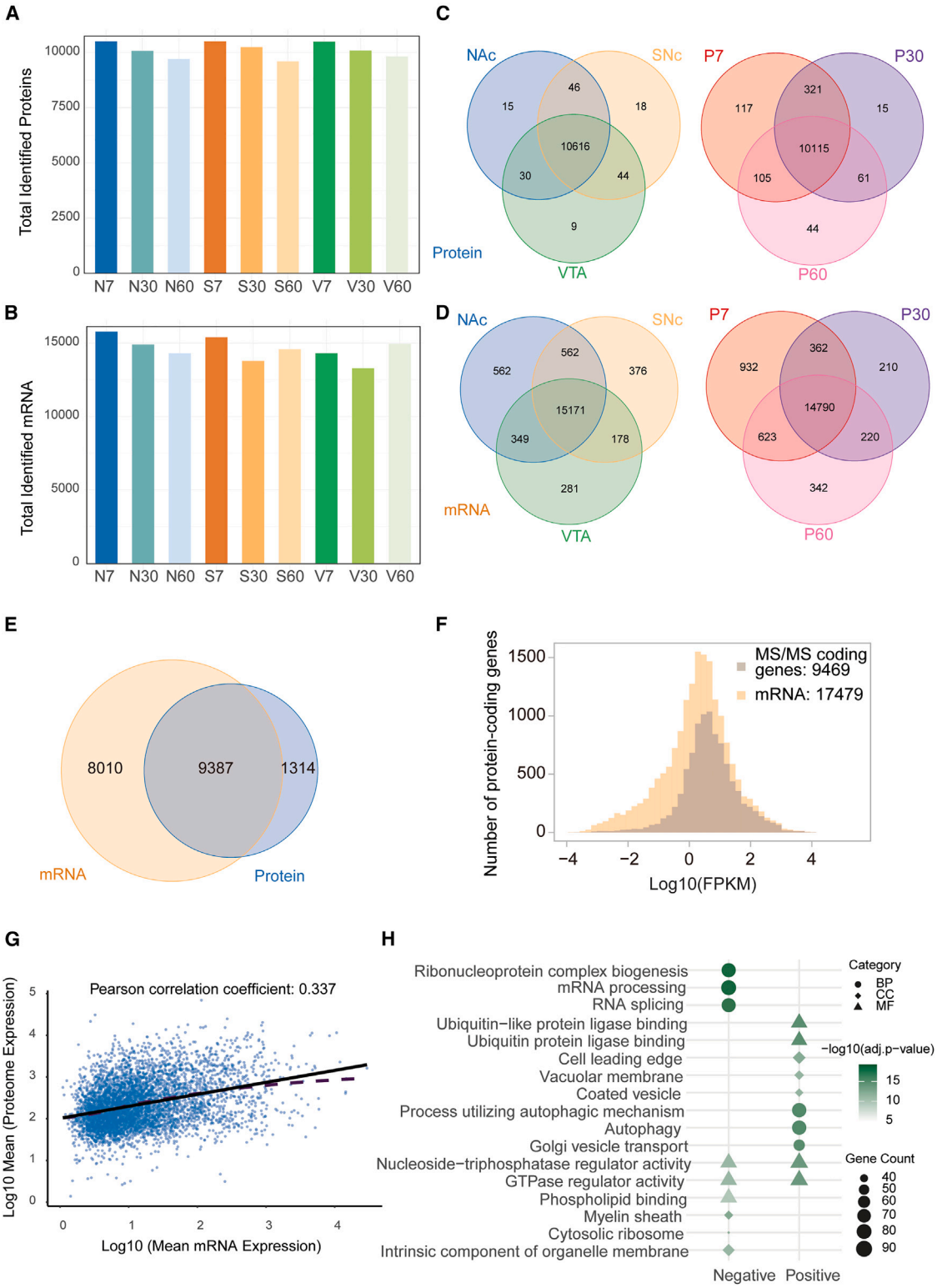

Figure 2. Integrative analysis of proteomic and transcriptomic datasets across different brain regions and developmental stages in DAT+ neurons

(A) Total number of identified proteins and (B) total number of identified mRNAs across various samples: NAc (N), SNc (S), and VTA (V) at different developmental stages (P7, P30, and P60), each bar represents the mean ± standard deviation.

(legend continued on next page)

to precisely isolate the DAT+ neurons (Figure 1C). The gating strategy employed during FACS ensured accurate selection, with validation through scatterplots showing the percentage of DAT+ cells in each sample. Additionally, we observed subtle differences in DAT+ cell populations between developmental stages and brain regions, with the proportion of DAT+ cells ranging from 0.5% to 4% across groups (Figures S1–S3; Table S1).

Following isolation, proteomic and transcriptomic analyses were performed using DIA-MS/MS and SMART-seq2 technologies, respectively (Figure 1C). This combined analysis revealed key molecular signatures, including Aldh1a1, allowing us to trace both proteome and transcriptome changes across developmental stages and brain regions.

Aldh1a1, a key gene encoding the aldehyde dehydrogenase 1a1 protein (ALDH1A1), is associated with the development of dopaminergic neurons. The differential expression of ALDH1A1 across regions and stages was confirmed through immunofluorescence staining, validating our omics-based findings and further supporting the biological relevance of ALDH1A1 in the maturation of DAT+ neurons.

Comparative overview and integrative analysis of proteomic and transcriptomic datasets in DAT+ neurons

After cell sorting, each brain region yielded approximately 11,000 DAT+ neurons, with 10,000 neurons used for proteomics and 1,000 neurons for transcriptomics, achieving a purity of 95%. Conventional proteomics sample preparation methods are inadequate for such small cell quantities. Therefore, we utilized an ultrasensitive trace sample proteomics method developed in our laboratory, enabling deep proteomic identification and quantification from micro-scale cell samples (Data S1.). This approach facilitates deep proteome analysis from trace biological samples, supporting biomedical applications, as traditional methods often lead to significant analyte loss during sample preparation.

From 10,000 DAT+ dopaminergic neurons, we consistently identified 8,000 to 10,000 proteins. The data indicated that within the same brain region, the total number of identified protein molecules shows a declining trend as development progresses (Figure 2A), whereas the transcriptome data do not exhibit a clear trend (Figure 2B).The Venn diagrams illustrated the results of proteomics and RNA-seq analyses across three specific brain regions (NAc, SNc, and VTA) and different developmental stages (P7, P30, and P60) (Figures 2C and 2D). In total, 10,616 proteins and 15,171 mRNAs were commonly identified across brain regions, while 10,115 proteins and 14,790 mRNAs were common across developmental stages.

The overlap between our proteomic and transcriptomic datasets includes 9,387 genes and proteins, demonstrating the depth of our analysis in trace samples (Figure 2E). The histogram compares the distribution of mRNA expression levels in genes identified by both RNA-seq and MS/MS datasets, showing that these genes generally exhibit higher mRNA expression levels compared to those uniquely detected by RNA-seq (Figure 2F).

The Pearson correlation coefficient of 0.337 between our proteomic and transcriptomic data reflects a moderate correlation between the transcriptome and proteome, implying complex interplay of transcriptional and translational processes within DA neurons (Figure 2G).[19] Detailed gene ontology (GO) enrichment analysis identified significant biological processes (BP), molecular functions (MF), and cellular components (CC) for positively and negatively correlated genes. This clarifies the roles of these genes in different BP and their translational regulatory mechanisms (Figure 2H). For positively correlated mRNA-protein pairs, significant BP include Golgi vesicle transport, ribonucleoprotein complex biogenesis, and protein folding. Molecular functions associated with these genes involve GTPase regulator activity, nucleoside-triphosphatase regulator activity, and ubiquitin protein ligase binding. Cellular components include the vacuolar membrane, cell leading edge, and coated vesicles, indicating roles in intracellular transport and protein folding. Negatively correlated pairs are enriched in BP such as ribonucleoprotein complex biogenesis and RNA splicing (including via transesterification reactions and spliceosome). Molecular functions include GTPase regulator activity, nucleoside-triphosphatase regulator activity, and mRNA binding. These genes are associated with cellular components such as the myelin sheath, cell leading edge, and cytosolic ribosome. This analysis highlights the complex interplay of transcriptional and translational processes in DAT+ neurons and their involvement in diverse biological functions and regulatory mechanisms (Table S2).

In-depth characterization of temporal protein expression alterations in DAT+ dopaminergic neurons

Proteomic data provide valuable insights into spatiotemporal dynamics, and this study focused on analyzing the proteome changes of DAT+ dopaminergic neurons across developmental stages (P7, P30, and P60). One-way ANOVA was used to identify proteins with significant expression changes across developmental stages. By combining data from three brain regions (NAc, SNc, and VTA) and applying a threshold of mean expression >1000 (representing the top 11.3% of protein abundance in at least one developmental stage), proteins with robust expression were selected for further analysis. This analysis identified 443 proteins with significant temporal expression changes ($p < 0.05$, log2 fold change > |1|). The complete list of significant proteins identified through one-way ANOVA is provided in Table S3.

Hierarchical clustering of these proteins revealed three distinct clusters, each characterized by distinct expression patterns

(C) Venn diagrams showing the overlap of identified proteins between NAc, SNc, and VTA (left), and across developmental stages (P7, P30, and P60) (right).
(D) Venn diagrams showing the overlap of identified mRNAs between NAc, SNc, and VTA (left), and across developmental stages (P7, P30, and P60) (right).
(E) Venn diagram showing the overlap between the identified mRNAs and proteins.
(F) Distribution of mRNA expression levels in genes identified by both RNA-seq and MS/MS datasets compared to those detected only by RNA-seq.
(G) Scatterplot showing the correlation between mean mRNA expression and mean proteome expression, with a Pearson correlation coefficient of 0.337 ($n = 3$); and (H) Functional enrichment analysis of gene categories with positive and negative correlations between mRNA and proteome expression. Categories are indicated by different shapes and sizes representing the gene count and significance levels. Categories include BP, CC, and MF.

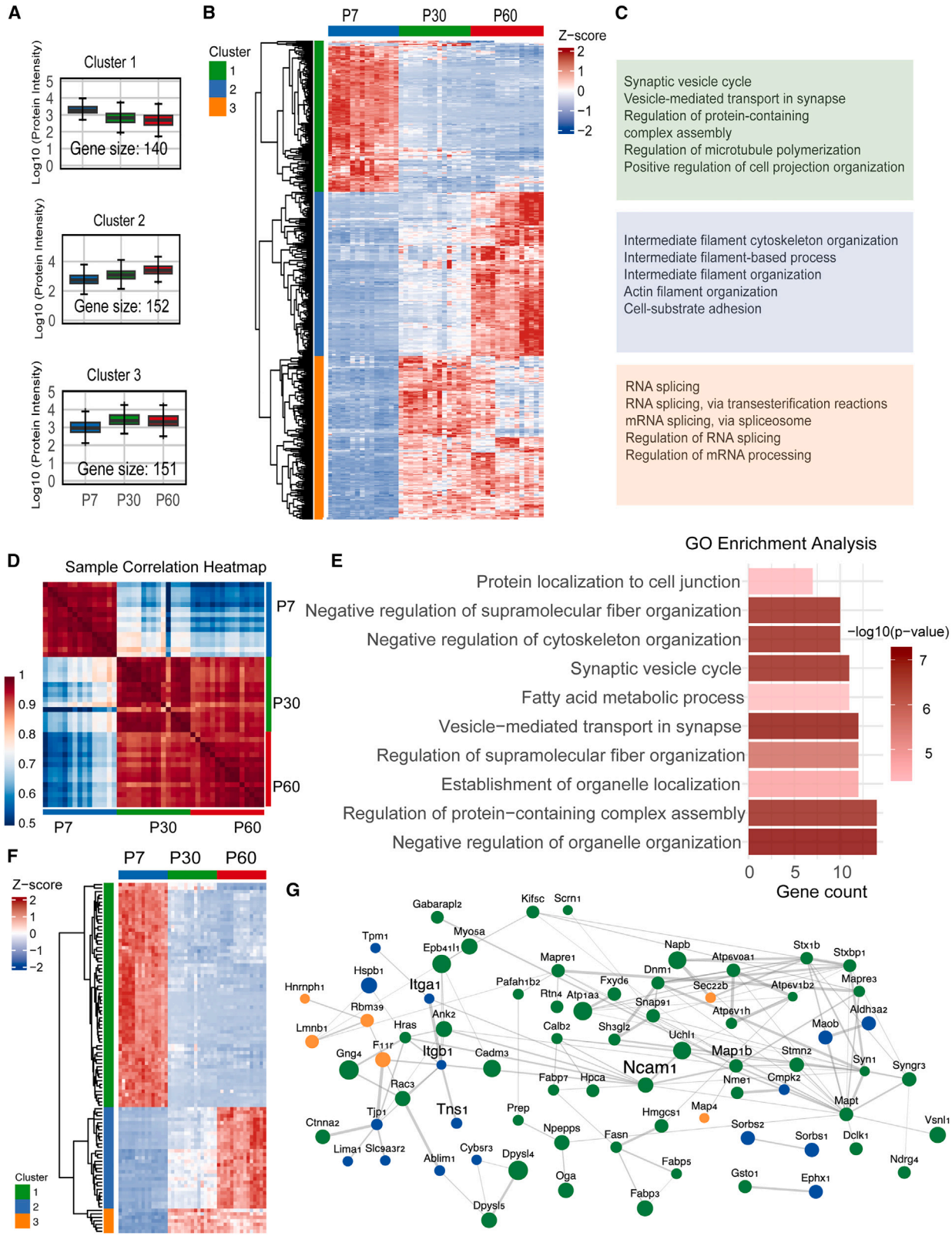

(legend on next page)

across developmental stages and associated BP (Figures 3A–3C). Cluster 1 contains 140 proteins that exhibited elevated expression at P7 compared to P30 and P60 and are primarily involved in synaptic functions and cognitive processes. Cluster 2 contains 152 proteins, showing significantly higher expression at P60, and are mainly involved in mRNA processing and RNA splicing. Cluster 3 contains 151 proteins showing higher expression at both P30 and P60, predominantly associated with intermediate filament cytoskeleton organization (Figure 3A). The heatmap of normalized protein expression levels (Z-scores) (Figure 3B) visually represents these distinct temporal expression patterns, highlighting the clear separation of developmental stages based on protein expression profiles.

Enriched GO terms for each cluster (Figure 3C; Table S4) underscore the specific BP predominant at each stage. Cluster 1 (green, P7) includes processes like the synaptic vesicle cycle and vesicle-mediated transport in synapse. This indicates that at the early developmental stage, DA neurons are highly active in synaptic function and cognitive processes. The focus is on forming and organizing synapses, which are crucial for establishing neuronal connections and communication. Cluster 2 (blue, P60) includes processes such as intermediate filament cytoskeleton organization and cell-substrate adhesion, emphasizing cytoskeletal organization and cell adhesion processes in mature DA neurons. These functions are essential for maintaining the structural integrity of neurons, facilitating stable connections, and supporting the complex architecture required for mature neuronal function. Cluster 3 (orange, P30 and P60) shows a significant focus on RNA processing and splicing mechanisms. This suggests that in the mid to late development stages, DA neurons are actively regulating gene expression at the post-transcriptional level, critical for producing the diverse set of proteins required for neuronal maturation and function.

The sample correlation heatmap (Figure 3D) underscores the high intra-stage correlation and distinct inter-stage differences, corresponding closely to the clusters identified in Figures 3A–3C. This heatmap highlights the clear distinctions in protein expression profiles between P7 and the other two stages, reinforcing the proteomic shifts observed across developmental stages.

Focusing on the top 100 differentially expressed proteins, GO enrichment analysis (Figure 3E; Table S5) revealed key BP at the protein level, such as protein localization to cell junctions, negative regulation of supramolecular fiber organization, and the synaptic vesicle cycle. This analysis illustrates the significant functional shifts in proteins involved in cytoskeleton structure; protein, complex, and organelle localization and organization; synaptic function and transmission; and metabolic processes during the development of DAT+ neurons. The heatmap (Figure 3F) showing protein expression differences across developmental stages further validates the dynamic changes observed in the proteomic landscape.

A detailed PPI network analysis of the top 100 differentially expressed proteins (Figure 3G) provided further insights into the molecular interactions at different developmental stages. For instance, at P60, proteins such as ITGA1, ITGB1, and TNS1 were significantly interconnected, highlighting their roles in cell adhesion, signal transduction, and cytoskeletal organization. ITGA1 (Integrin alpha-1) and ITGB1 (Integrin beta-1) are integral in forming integrin complexes that mediate cell-extracellular matrix interactions, crucial for cellular communication and structural integrity.[20,21] TNS1 (Tensin-1) plays a pivotal role in linking integrins to the actin cytoskeleton, facilitating cell migration and adhesion.[22] Conversely, the early developmental stage (P7) featured a cluster of proteins involved in synaptic functions and cellular processes, such as MAPT, MAP1B, and NCAM1. MAPT (tau) is crucial for microtubule stability and axonal growth,[23,24] MAP1B is essential for cytoskeletal dynamics and neuronal development,[25] and NCAM1 is critical for neural cell adhesion and synaptic plasticity.[26,27] The prominence of these proteins during the neonatal stage highlights the intensive cellular activities essential for rapid neuronal proliferation and differentiation.

There are extensive interconnections between proteins significantly upregulated at P60 and those at P7, suggesting a complex interplay between early and mature neuronal states. These interactions underscore the importance of continuous molecular interactions throughout neuronal development, facilitating the transition from proliferative to mature functional states.

Overall, our findings elucidate the temporal dynamics of protein expression in DAT+ dopaminergic neurons, highlighting distinct molecular mechanisms at different developmental stages. These insights provide a comprehensive understanding of the complex regulatory networks governing neuronal development and function at the protein level. This foundational knowledge is crucial for future studies aimed at understanding neurodevelopmental and neurodegenerative diseases, potentially informing therapeutic interventions.

Spatial specificity of the DAT+ dopaminergic neurons proteome across brain regions

To further investigate the spatial specificity of DAT+ dopaminergic neurons, we examined their proteomic profiles across three brain regions—NAc, SNc, and VTA—at critical developmental stages

Figure 3. Temporal dynamics of protein expression in DAT+ neurons across developmental stages

(A) Boxplots displaying the size of the characteristic protein clusters of different developmental stages (P7, P30, and P60) as well as expression levels of proteins.

(B) Heatmap showing normalized protein expression (Z-scores) across developmental stages, with significant proteins ($p < 0.05$, log2 fold change > |1|, mean expression >1000) included.

(C) The top 5 GO terms enriched in each cluster.

(D) Sample correlation heatmap across developmental stages.

(E) GO enrichment bar plot for the top 100 differentially expressed proteins, illustrating the most significantly enriched biological processes.

(F) Heatmap of the top 100 differentially expressed proteins, categorized into three clusters.

(G) PPI network of the top 100 proteins, color-coded by cluster, with key proteins like NCAM1 highlighted for their central roles.

One-way ANOVA, variable: developmental stage, $p < 0.05$, $N = 5$; Tukey HSD post hoc test for pairwise comparisons.

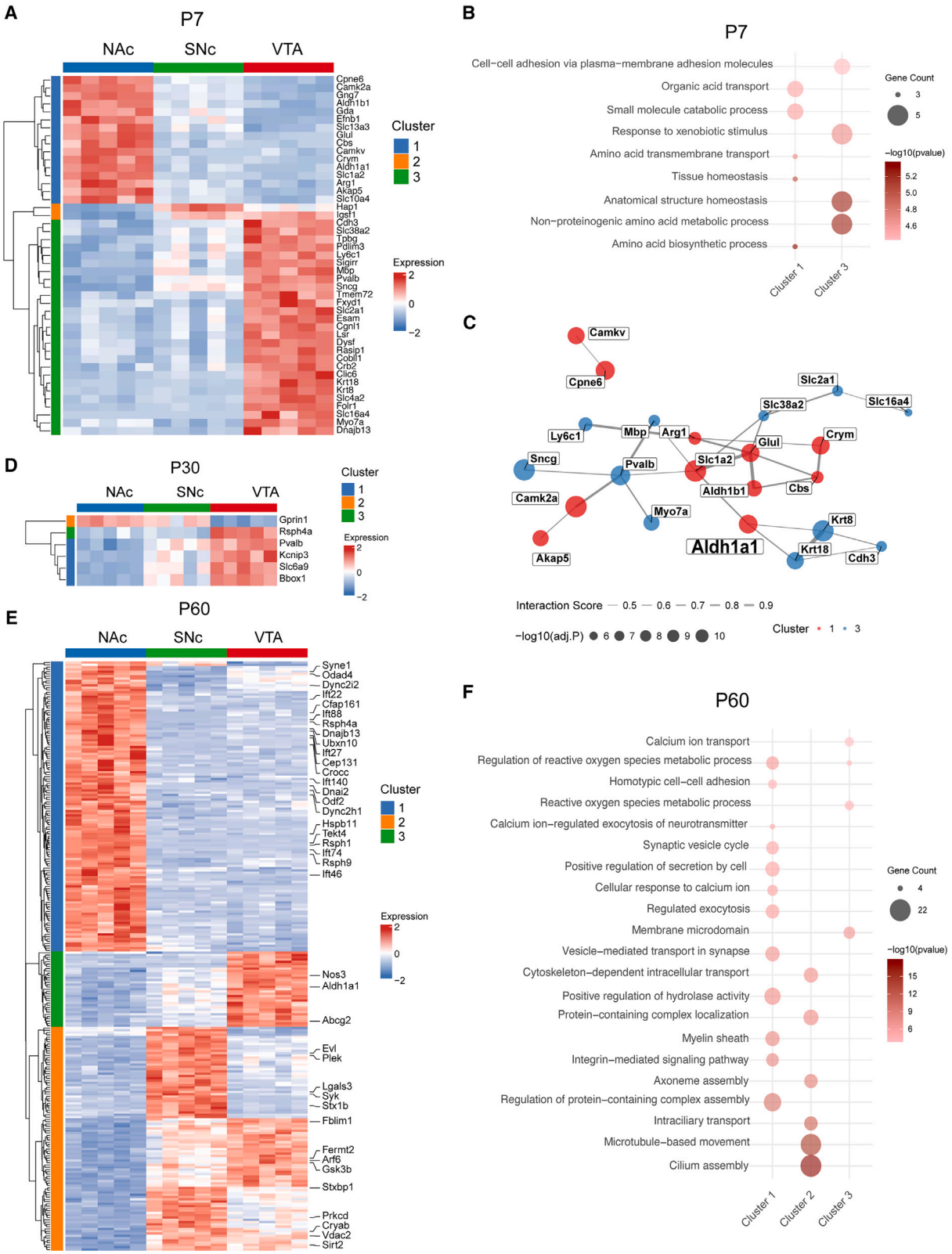

(legend on next page)

(P7, P30, and P60). We applied one-way ANOVA ($p < 0.05$, log2 fold change > |1|) to identify proteins with significant expression differences among the regions. Distinct clusters of differentially expressed proteins were visualized through heatmaps for P7, P30, and P60 (Figures 4A, 4D, and 4E), revealing unique molecular features in each region at different stages. Biological replicates ($n = 5$ per group) were used for statistical analysis. The complete lists of significant proteins identified through one-way ANOVA for spatial specificity at P7, P30, and P60 are provided in Tables S6, S7, and S8, respectively.

At P7, Cluster 1 proteins, upregulated in the NAc, are enriched in processes such as organic acid transport and small molecule catabolic process, indicating its role in maintaining metabolic functions (Figure 4B; Table S9). The key proteins include ALDH1A1 and SLC1A2. ALDH1A1 (Aldehyde Dehydrogenase 1 Family Member A1) detoxifies aldehydes, which are byproducts of dopamine metabolism, thereby supporting dopaminergic neuron health and protecting against oxidative stress.[28–30] SLC1A2 (glutamate transporter EAAT2) is essential for glutamate reuptake from the synaptic cleft, preventing excitotoxicity and maintaining synaptic function.[31,32] These processes are critical for sustaining neuronal function and facilitating intercellular communication, underscoring the metabolic and structural specialization of the NAc during early development.

Cluster 3, predominantly upregulated in the VTA, is enriched in processes such as responses to xenobiotic stimuli, anatomical structure homeostasis, and amino acid metabolic and biosynthetic processes. These functions indicate involvement in detoxification, structural maintenance, and protein synthesis. The key proteins, such as PVALB and MBP, are essential for synaptic function and myelination. PVALB (parvalbumin) is a calcium-binding protein critical for the precise timing of neurotransmission,[33] while MBP (myelin basic protein) is crucial for forming and stabilizing myelin sheaths around axons, ensuring efficient neural signal transmission.[34] The PPI network analysis at P7 (Figure 4C) provides a detailed view of interactions among region-specific proteins. Key proteins such as ALDH1A1, SLC1A2, GLUL, and ARG1, central to the NAc network, highlight the metabolic and neurotransmitter regulation critical for dopaminergic signaling. ALDH1A1 and ALDH1B1, involved in aldehyde metabolism, play essential roles in detoxifying neural tissues from dopamine metabolism byproducts. SLC1A2 and GLUL, key players in glutamate metabolism, underscore the interplay between dopaminergic and glutamatergic signaling, reflecting the intricate balance of neurotransmitter systems necessary for functional neural circuits.

In P30, the heatmap indicates small changes in protein expression profiles across the brain regions (Figure 4D). Proteins RPS4HA and KCNIP3 show distinct expression patterns, playing critical roles in ribosomal function and ion channel regulation, respectively, suggesting significant cellular adaptations during this developmental stage.

In P60, the heatmap reveals more pronounced differential expression patterns (Figure 4E). Cluster 1 proteins, upregulated in the NAc, include SYNE1 and IFT22, which are involved in structural integrity and intraflagellar transport, respectively. SYNE1 (spectrin repeat containing nuclear envelope protein 1) is crucial for maintaining nuclear structure and cellular integrity,[35] while IFT22 (intraflagellar transport 22) is involved in the biogenesis of cilia and flagella, critical for cellular signaling and movement.[36] Cluster 3 proteins, predominantly upregulated in the VTA, include ALDH1A1, highlighting its continued importance in metabolic processes. Cluster 2 proteins, significantly downregulated in the NAc, include FBLIM1 and LGALS3, which are involved in cell adhesion and immune response.[37,38]

GO enrichment analysis at P60 (Figure 4F; Table S10) further elucidates the complexity of the dopaminergic system at this mature stage. Cluster 1 proteins are involved in processes such as cilium assembly, intracellular transport, and microtubule-based movement, highlighting the critical roles of NAc-enriched processes in cellular organization and transport mechanisms. Cluster 2 proteins are associated with the regulation of protein-containing complex assembly, integrin-mediated signaling pathways, and vesicle-mediated transport in synapse, emphasizing VTA-specific pathways in maintaining synaptic transmission and neuronal connectivity. Cluster 3 proteins are involved in calcium ion transport, regulation of reactive oxygen species metabolic processes, and positive regulation of secretion by cells, indicating their roles in signal transduction and cellular homeostasis.

This comprehensive analysis of the spatial-temporal protein expression dynamics within DAT+ dopaminergic neurons reveals distinct molecular mechanisms governing neuronal development and specialization. Central proteins like ALDH1A1, SLC1A2, and GLUL play pivotal roles in critical metabolic and signaling pathways, reflecting their importance in maintaining the health and function of DAT+ neurons. Our findings provide insights into the molecular mechanisms underlying the development and maturation of dopaminergic neurons in different brain regions, offering a foundation for understanding neurodevelopmental and neurodegenerative diseases.

Figure 4. The protein expression signatures and networks reflect the spatial specificity of DAT+ neurons in different developmental stages

(A) Heatmaps display spatially distinct protein expression in NAc, SNc, and VTA at P7, identifying clusters based on significant changes ($p < 0.05$, log2 fold change > |1|).

(B) GO analysis at P7 reveals enriched biological processes for each cluster.

(C) PPI network at P7 illustrates interactions within the NAc, SNc, and VTA, highlighting key proteins and their connectivity, with clusters indicated by different colors.

(D) Heatmaps display spatially distinct protein expression in NAc, SNc, and VTA at P30, identifying clusters based on significant changes ($p < 0.05$, log2 fold change > |1|).

(E) Heatmaps display spatially distinct protein expression in NAc, SNc, and VTA at P60, identifying clusters based on significant changes ($p < 0.05$, log2 fold change > |1|).

(F) GO analysis at P60 reveals enriched biological processes for each cluster.

One-way ANOVA, variable: brain regions, $p < 0.05$, $N = 5$; Tukey HSD post hoc test for pairwise comparisons.

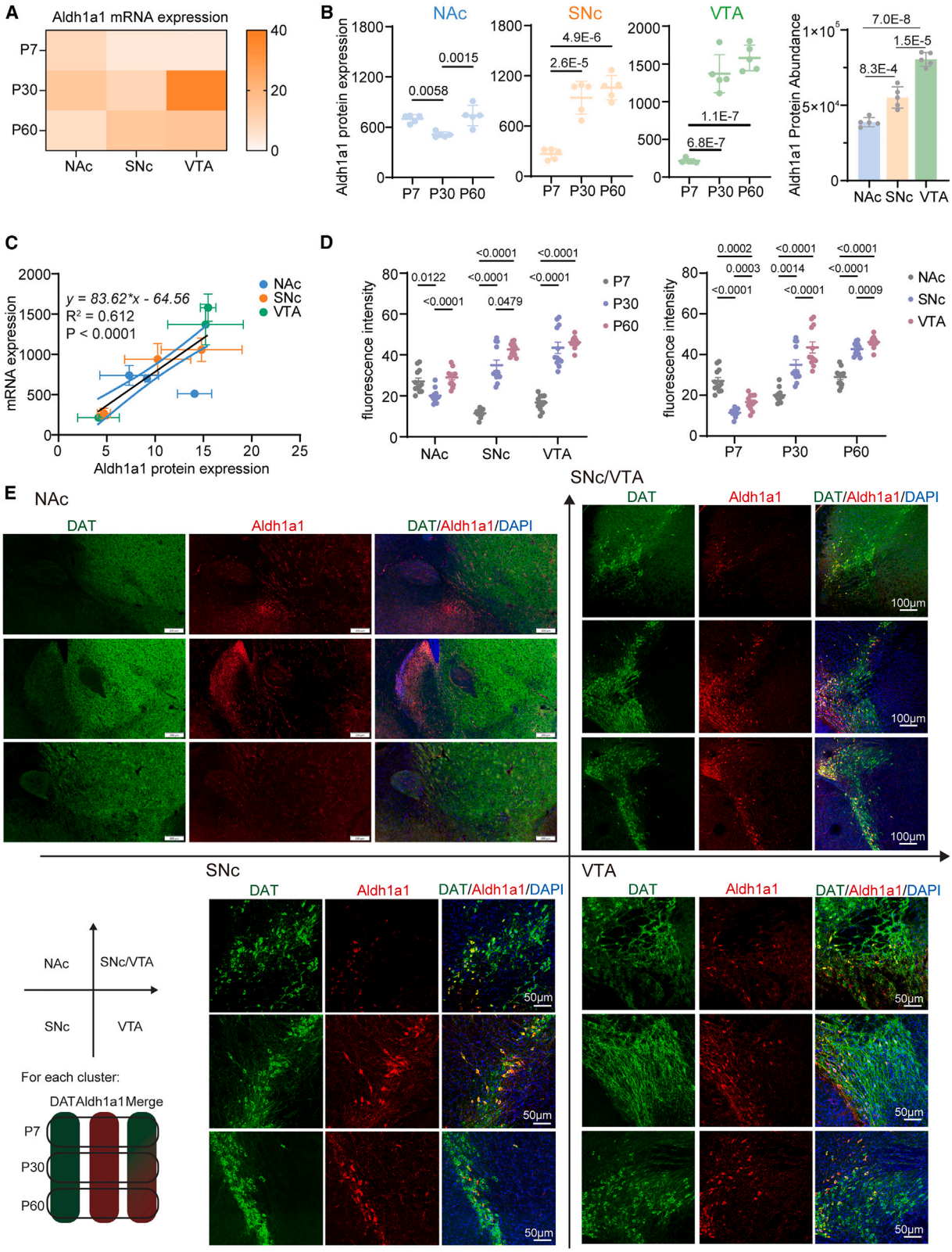

(legend on next page)

ALDH1A1 expression is strongly associated with sub-clusters of dopaminergic neurons

Transcriptomics and proteomics have revealed the spatiotemporal expression heterogeneity of multiple molecules, including ALDH1A1, which was validated in this study. Firstly, the heatmap shows the expression of *Adh1a1* mRNA in three different brain regions (NAc, SNc, and VTA) across developmental stages (P7, P30, and P60). The *Adh1a1* mRNA levels increased over time in all brain regions, particularly in the SNc and VTA (Figure 5A). Similarly, ALDH1A1 protein levels showed a parallel trend, with increasing expression over time, particularly in the SNc and VTA (Figure 5B).

Correlation analysis revealed a significant positive relationship (R^2 = 0.612) between *Adh1a1* mRNA and ALDH1A1 protein expression, demonstrating consistency between transcription and translation (Figure 5C). The localization of ALDH1A1 protein was further confirmed by immunofluorescence experiments, which highlighted its expression in DAT+ neurons across developmental stages (P7, P30, P60) and brain regions (NAc, SNc, VTA) (Figure 5E). Quantitative analysis of fluorescence intensity revealed a progressive increase in ALDH1A1 expression across all regions, with the most pronounced changes observed in the VTA (Figure 5D).

Notably, ALDH1A1 is expressed in a specific sub-population of DAT+ neurons. The dynamic changes in ALDH1A1 expression, particularly the significant increase in the VTA, suggest that ALDH1A1+/DAT+ neurons may contribute to region-specific developmental and functional adaptations. Further research is warranted to explore the biological significance of these neurons and their potential roles in neuronal function.

DISCUSSION

Our comprehensive analysis of DAT+ dopaminergic (DA) neurons reveals significant molecular diversity and dynamic changes across key developmental stages in the NAc, SNc, and VTA. These findings highlight distinct temporal expression patterns and regulatory mechanisms that are essential for DA neuron development. The moderate Pearson correlation coefficient between mRNA and protein expression underscores the complexity of transcriptional and translational regulation, where post-transcriptional and post-translational modifications play crucial roles.[19] Enriched BP, such as the synaptic vesicle cycle and protein folding, among correlated gene-protein pairs provide deeper insights into the molecular functions and cellular components involved in DA neuron maturation.

The temporal increase in ALDH1A1 expression, particularly in the SNc and VTA, underscores its involvement in retinoic acid production, neuronal development, and specific physiological functions.[29] Recent studies have linked ALDH1A1 to neuroprotective mechanisms under oxidative stress, which are relevant to Parkinson's disease pathology.[30] Validation through proteomics, transcriptomics, and immunofluorescence staining further supports its potential as a molecular marker for DA neuron maturation. The dynamic expression of ALDH1A1 suggests its role in differentiation, maintenance, and neuroprotection, offering new perspectives on its functionality and resilience against neurodegenerative processes.

Our spatial analysis uncovers distinct molecular signatures and functional specializations of DAT+ neurons across the NAc, SNc, and VTA. Proteins involved in metabolic processes, synaptic function, and cellular organization exhibit region-specific expression patterns. For example, ALDH1A1 and SLC1A2 are prominently expressed in the NAc, underscoring their critical roles in maintaining metabolic homeostasis. In contrast, PVALB and MBP are highly expressed in the VTA, emphasizing their importance in synaptic function and myelination. These findings align with molecular diversity reported in single-cell RNA sequencing studies of midbrain DA neurons[10] and advancements in spatial transcriptomics, offering deeper insights into the spatial heterogeneity of dopaminergic neurons.

Our multi-omics dataset provides critical insights into the molecular mechanisms governing DA neuron development and function. Understanding the spatiotemporal dynamics of protein and gene expression in DAT+ neurons is fundamental to elucidating the pathophysiology of neurodevelopmental and neurodegenerative disorders. Furthermore, insights into the molecular diversity of DA neurons can inform the development of targeted interventions for conditions such as schizophrenia and addiction, where dopaminergic signaling plays a central role[5,4]. Future research, leveraging advances in multi-omics technologies, will be crucial in further unraveling the complex biology of DA neurons and facilitating the design of targeted therapies for neurodevelopmental and neurodegenerative diseases.

Limitations of the study

This study focuses on postnatal stages (P7, P30, P60) and three brain regions (NAc, SNc, VTA), leaving other temporal windows and regions unexplored. Although advanced multi-omics

Figure 5. Transcriptomic and proteomic analysis revealed ALDH1A1 expression as strongly associated with specific brain regions and developmental stages

(A) Heatmap showing Aldh1a1 mRNA expression levels across different developmental stages (P7, P30, P60) in three brain regions: NAc, SNc, and VTA. (N = 3).

(B) ALDH1A1 protein expression level in the NAc, SNc, and VTA at P7, P30, and P60, revealed significant spatiotemporal difference. Statistical significance between stages is indicated. One-way ANOVA was used to analyze differences between developmental stages, with Tukey HSD post hoc test for pairwise comparisons. Significant p values are indicated (For NAc, p = 0.0012; for SNc, $p < 0.0001$; for VTA, $p < 0.0001$, N = 5).

(C) Linear regression fittings of ALDH1A1 protein expression versus mRNA transcription levels, demonstrating a significantly positive correlation among all groups. ($p < 0.0001$) (D) Fluorescence intensity of ALDH1A1+/DAT+ cells in different brain regions and developmental stages. Two-way repeated measures ANOVA was applied to assess the effects of brain region and developmental stage, with significant differences observed for both factors ($p < 0.0001$ for brain region x developmental stage, N = 5).

(E) Immunofluorescent staining of DAT+ neurons (green) and ALDH1A1 protein (red) in brain sections of NAc (top left), SNc/VTA (top right), SNc (bottom left), and VTA (bottom right) across different developmental stages (P7, P30, and P60). Scale bars represent 200 μm (top left), 100 μm (top right), 50 μm (bottom left and right).

techniques were applied, further *in vivo* investigations, including behavioral assays or disease models, are essential to comprehensively elucidate the biological significance and functional implications of these findings. Expanding the temporal and spatial scopes in future studies, along with leveraging human-derived models, may enhance the translational potential of this research.

RESOURCE AVAILABILITY

Lead contact

For further information and requests for resources and reagents, please contact Huali Shen (shenhuali@fudan.edu.cn).

Materials availability

This study did not generate new unique reagents.

Data and code availability

- The proteomics and transcriptomics data generated in this study have been deposited at the ProteomeXchange Consortium and GEO. The accession numbers are iProX: PXD055527 and GEO: GSE285556. These data are publicly available for access and are listed in the key resources table.
- This paper does not report original code.
- Any additional information required to reanalyze the data reported in this paper is available from the lead contact upon request.

ACKNOWLEDGMENTS

This work was supported by the National Key Research and Development Program (2021YFA1301601), the Science and Technology Innovation 2030 Major Projects (2022ZD0211600), the National Natural Science Foundation of China (81827901 and 82272174), the Science and Technology Innovation Action Plan of STCSM (22S31901900) and the innovative research team of high-level local university in Shanghai, as well as the NHC Key Laboratory of Glycoconjugates Research. We thank the proteomics and mass spectrometry platform of Institutes of Biomedical Sciences, Fudan University.

The manuscript is dedicated to Professor P.Y. (1949–2021).

AUTHOR CONTRIBUTIONS

H.Z. and P.C. contributed equally to this work; they designed and performed the experiments, analyzed the data, and prepared the manuscript. X.G. assisted in protein preparation. Z. H. directed animal tissue dissection. P. Y. and H. S. directed the project. H. S. also assisted in the manuscript preparation.

DECLARATION OF INTERESTS

The authors declare no competing interests.

STAR★METHODS

Detailed methods are provided in the online version of this paper and include the following:

- KEY RESOURCES TABLE
- EXPERIMENTAL MODEL AND STUDY PARTICIPANT DETAILS
  - Animals
- METHOD DETAILS
  - Animal tissue dissection and neuron dissociation
  - Protein sample preparation based on SMID method
  - High pH reverse phase separation and mass spectrometry
  - RNA-seq
  - Immunofluorescence staining
- QUANTIFICATION AND STATISTICAL ANALYSIS

SUPPLEMENTAL INFORMATION

Supplemental information can be found online at https://doi.org/10.1016/j.isci.2025.112115.

Received: July 25, 2024
Revised: October 9, 2024
Accepted: February 24, 2025
Published: February 27, 2025

REFERENCES

1. Björklund, A., and Dunnett, S.B. (2007). Dopamine neuron systems in the brain: an update. Trends Neurosci. *30*, 194–202.
2. Lammel, S., Lim, B.K., and Malenka, R.C. (2014). Reward and aversion in a heterogeneous midbrain dopamine system. Neuropharmacology *76 Pt B*, 351–359.
3. Smidt, M.P., and Burbach, J.P.H. (2007). How to make a mesodiencephalic dopaminergic neuron. Nat. Rev. Neurosci. *8*, 21–32.
4. Russo, S.J., and Nestler, E.J. (2013). The brain reward circuitry in mood disorders. Nat. Rev. Neurosci. *14*, 609–625.
5. Morales, M., and Margolis, E.B. (2017). Ventral tegmental area: cellular heterogeneity, connectivity and behaviour. Nat. Rev. Neurosci. *18*, 73–85.
6. Poulin, J.-F., Gaertner, Z., Moreno-Ramos, O.A., and Awatramani, R. (2020). Classification of Midbrain Dopamine Neurons Using Single-Cell Gene Expression Profiling Approaches. Trends Neurosci. *43*, 155–169.
7. Tiklová, K., Björklund, Å.K., Lahti, L., Fiorenzano, A., Nolbrant, S., Gillberg, L., Volakakis, N., Yokota, C., Hilscher, M.M., Hauling, T., et al. (2019). Single-cell RNA sequencing reveals midbrain dopamine neuron diversity emerging during mouse brain development. Nat. Commun. *10*, 581.
8. Jerber, J., Seaton, D.D., Cuomo, A.S.E., Kumasaka, N., Haldane, J., Steer, J., Patel, M., Pearce, D., Andersson, M., Bonder, M.J., et al. (2021). Population-scale single-cell RNA-seq profiling across dopaminergic neuron differentiation. Nat. Genet. *53*, 304–312.
9. Hobson, B.D., Choi, S.J., Mosharov, E.V., Soni, R.K., Sulzer, D., and Sims, P.A. (2022). Subcellular proteomics of dopamine neurons in the mouse brain. Elife *11*, e70921.
10. La Manno, G., Gyllborg, D., Codeluppi, S., Nishimura, K., Salto, C., Zeisel, A., Borm, L.E., Stott, S.R.W., Toledo, E.M., Villaescusa, J.C., et al. (2016). Molecular diversity of midbrain development in mouse, human, and stem cells. Cell *167*, 566–580.e19.
11. Hegarty, S.V., Sullivan, A.M., and O'Keeffe, G.W. (2013). Midbrain dopaminergic neurons: A review of the molecular circuitry that regulates their development. Dev. Biol. *379*, 123–138.
12. Kadkhodaei, B., Alvarsson, A., Schintu, N., Ramsköld, D., Volakakis, N., Joodmardi, E., Yoshitake, T., Kehr, J., Decressac, M., Björklund, A., et al. (2013). Transcription factor Nurr1 maintains fiber integrity and nuclear-encoded mitochondrial gene expression in dopamine neurons. Proc. Natl. Acad. Sci. USA *110*, 2360–2365.
13. Wang, Y., Chen, X., Wang, Y., Li, S., Cai, H., and Le, W. (2021). The essential role of transcription factor Pitx3 in preventing mesodiencephalic dopaminergic neurodegeneration and maintaining neuronal subtype identities during aging. Cell Death Dis. *12*, 1008.
14. Farassat, N., Costa, K.M., Stojanovic, S., Albert, S., Kovacheva, L., Shin, J., Egger, R., Somayaji, M., Duvarci, S., Schneider, G., and Roeper, J. (2019). In vivo functional diversity of midbrain dopamine neurons within identified axonal projections. Elife *8*, e48408.
15. Poulin, J.-F., Caronia, G., Hofer, C., Cui, Q., Helm, B., Ramakrishnan, C., Chan, C.S., Dombeck, D.A., Deisseroth, K., and Awatramani, R. (2018). Mapping projections of molecularly defined dopamine neuron subtypes using intersectional genetic approaches. Nat. Neurosci. *21*, 1260–1271.
16. Lammel, S., Lim, B.K., Ran, C., Huang, K.W., Betley, M.J., Tye, K.M., Deisseroth, K., and Malenka, R.C. (2012). Input-specific control of reward and aversion in the ventral tegmental area. Nature *491*, 212–217.

17. Yang, S., Xiong, Y., Du, Y., Wang, Y.J., Zhang, L., Shen, F., Liu, Y.J., Liu, X., and Yang, P. (2021). Ultrasensitive trace sample proteomics unraveled the protein remodeling during mesenchymal–amoeboid transition. Anal. Chem. *94*, 768–776.

18. Picelli, S., Björklund, Å.K., Björklund, A.K., Winberg, G., Sagasser, S., and Sandberg, R. (2014). Full-length RNA-seq from single cells using Smart-seq2. Nat. Protoc. *9*, 171–181.

19. Sharma, K., Schmitt, S., Bergner, C.G., Tyanova, S., Kannaiyan, N., Manrique-Hoyos, N., Kongi, K., Cantuti, L., Hanisch, U.K., Philips, M.A., et al. (2015). Cell type–and brain region–resolved mouse brain proteome. Nat. Neurosci. *18*, 1819–1831.

20. Arnaout, M.A., Mahalingam, B., and Xiong, J.-P. (2005). Integrin structure, allostery, and bidirectional signaling. Annu. Rev. Cell Dev. Biol. *21*, 381–410.

21. Pang, X., He, X., Qiu, Z., Zhang, H., Xie, R., Liu, Z., Gu, Y., Zhao, N., Xiang, Q., and Cui, Y. (2023). Targeting integrin pathways: mechanisms and advances in therapy. Signal Transduct. Target. Ther. *8*, 1.

22. Lo, S.H., Weisberg, E., and Chen, L.B. (1994). Tensin: a potential link between the cytoskeleton and signal transduction. Bioessays *16*, 817–823.

23. Wang, Y., and Mandelkow, E. (2016). Tau in physiology and pathology. Nat. Rev. Neurosci. *17*, 22–35.

24. Beevers, J.E., Lai, M.C., Collins, E., Booth, H.D.E., Zambon, F., Parkkinen, L., Vowles, J., Cowley, S.A., Wade-Martins, R., and Caffrey, T.M. (2017). MAPT genetic variation and neuronal maturity alter isoform expression affecting axonal transport in iPSC-derived dopamine neurons. Stem Cell Rep. *9*, 587–599.

25. Yang, M., Wu, M., Xia, P., Wang, C., Yan, P., Gao, Q., Liu, J., Wang, H., Duan, X., and Yang, X. (2012). The role of microtubule-associated protein 1B in axonal growth and neuronal migration in the central nervous system. Neural Regen. Res. *7*, 842–848.

26. Westphal, N., Theis, T., Loers, G., Schachner, M., and Kleene, R. (2017). Nuclear fragments of the neural cell adhesion molecule NCAM with or without polysialic acid differentially regulate gene expression. Sci. Rep. *7*, 13631.

27. Cao, J.-P., Wang, H.J., Yu, J.K., Yang, H., Xiao, C.H., and Gao, D.S. (2008). Involvement of NCAM in the effects of GDNF on the neurite outgrowth in the dopamine neurons. Neurosci. Res. *61*, 390–397.

28. Sgobio, C., Wu, J., Zheng, W., Chen, X., Pan, J., Salinas, A.G., Davis, M.I., Lovinger, D.M., and Cai, H. (2017). Aldehyde dehydrogenase 1–positive nigrostriatal dopaminergic fibers exhibit distinct projection pattern and dopamine release dynamics at mouse dorsal striatum. Sci. Rep. *7*, 5283.

29. Doorn, J.A., Florang, V.R., Schamp, J.H., and Vanle, B.C. (2014). Aldehyde dehydrogenase inhibition generates a reactive dopamine metabolite autotoxic to dopamine neurons. Parkinsonism Relat. Disord. *20*, S73–S75.

30. Calleja, L.F., Yoval-Sánchez, B., Hernández-Esquivel, L., Gallardo-Pérez, J.C., Sosa-Garrocho, M., Marín-Hernández, Á., Jasso-Chávez, R., Macías-Silva, M., and Salud Rodríguez-Zavala, J. (2021). Activation of ALDH1A1 by omeprazole reduces cell oxidative stress damage. FEBS J. *288*, 4064–4080.

31. O'Donovan, S.M., Sullivan, C.R., and McCullumsmith, R.E. (2017). The role of glutamate transporters in the pathophysiology of neuropsychiatric disorders. NPJ Schizophr *3*, 32.

32. Veldic, M., Millischer, V., Port, J.D., Ho, A.M.C., Jia, Y.F., Geske, J.R., Biernacka, J.M., Backlund, L., McElroy, S.L., Bond, D.J., et al. (2019). Genetic variant in SLC1A2 is associated with elevated anterior cingulate cortex glutamate and lifetime history of rapid cycling. Transl. Psychiatry *9*, 149.

33. Nahar, L., Delacroix, B.M., and Nam, H.W. (2021). The role of parvalbumin interneurons in neurotransmitter balance and neurological disease. Front. Psychiatry *12*, 679960.

34. Nave, K.-A., and Werner, H.B. (2014). Myelination of the nervous system: mechanisms and functions. Annu. Rev. Cell Dev. Biol. *30*, 503–533.

35. Zhou, C., Rao, L., Shanahan, C.M., Zhang, Q., and Yu, Q. (2018). Nesprin-1/2: roles in nuclear envelope organisation, myogenesis and muscle disease. Biochem. Soc. Trans. *46*, 311–320.

36. Xue, B., Zhang, Y., Yu, X., Zhang, T., and Pan, X.Y. (2020). Intraflagellar transport protein RABL5/IFT22 recruits the BBSome to the basal body through the GTPase ARL6/BBS3. Proc. Natl. Acad. Sci. *117*, 2496–2505.

37. Xiao, G., Cheng, H., Cao, H., Chen, K., Tu, Y., Yu, S., Jiao, H., Yang, S., Im, H.J., Chen, D., et al. (2012). Critical role of filamin-binding LIM protein 1 (FBLP-1)/migfilin in regulation of bone remodeling. J. Biol. Chem. *287*, 21450–21460.

38. Soares, L.C., Al-Dalahmah, O., Hillis, J., Young, C.C., Asbed, I., Sakaguchi, M., O'Neill, E., and Szele, F.G. (2021). Novel galectin-3 roles in neurogenesis, inflammation and neurological diseases. Cells *10*, 3047.

STAR★METHODS

KEY RESOURCES TABLE

REAGENT or RESOURCE	SOURCE	IDENTIFIER
Antibodies		
direct-labeled anti-Dopamine Transporter (DAT)-FITC antibody	Alomone Labs	Cat# AMT-003-F; RRID: AB_2827324
Rabbit Anti-Dopamine Transporter	Abcam	Cat#ab184451; RRID: AB_2890225
Goat Anti-ALDH1A1 Antibody	R&D Systems	Cat# AF5868; RRID: AB_1964500
Donkey Anti-Rabbit IgG H&L (Alexa Fluor® 488)	Abcam	Cat# ab150073; RRID: AB_2636877
Donkey Anti-Goat IgG H&L (Alexa Fluor® 594)	Abcam	Cat# ab150132; RRID: AB_2810222
Deposited data		
Spatiotemporal Proteomic and Transcriptomic Landscape of DAT+ Dopaminergic Neurons Development and Function	iProX	PXD055527
Spatiotemporal Proteomic and Transcriptomic Landscape of DAT+ Dopaminergic Neurons Development and Function	GEO	GSE285556
Software and algorithms		
Spectronaut	Biognosys	Version 16
Other		
Adult Mouse Dissociation Kit	Miltenyi Biotech	130-096-731
Myelin Removal Beads II	Miltenyi Biotech	130-096-731
Neural Tissue Dissociation Kit (P)	Miltenyi Biotech	130-092-628

EXPERIMENTAL MODEL AND STUDY PARTICIPANT DETAILS

Animals

Male C57BL/6 mice aged P7 (infancy), P30 (juvenile), and P60 (adult) were used in this study. The mice were housed in the Experimental Animal Center of Fudan University under standard laboratory conditions, including a controlled environment maintained at 24 ± 2°C, 60 ± 5% humidity, and a 12-hour light/dark cycle at 100 lux. Food and water were provided *ad libitum*. All animal experiments were approved by the Experimental Animal Ethics Committee of Fudan University (Number: DSF-2024-043).

METHOD DETAILS

Animal tissue dissection and neuron dissociation

Brain tissue samples were collected from the substantia nigra pars compacta (SNc), ventral tegmental area (VTA), and nucleus accumbens (NAc) of C57BL/6 mice. Neurons were dissociated using fluorescence-activated cell sorting (FACS) with anti-DAT-FITC antibodies.

Protein sample preparation based on SMID method

Proteins were prepared using the single-pot and miniaturized in-solution digestion (SMID) method. Cells were lysed using ammonium bicarbonate (ABC) solution with RapiGest, followed by reduction with tris(2-carboxyethyl) phosphine (TCEP) and alkylation with chloroacetamide (CAA). Digestion was performed with trypsin and Lys-C, and peptides were purified using ZipTip columns.

High pH reverse phase separation and mass spectrometry

The peptide mixture was resuspended in buffer A (20 mM ammonium formate in water, pH 10.0) and subjected to high pH reverse-phase separation using an XBridge C18 column (4.6 mm x 250 mm, 5 μm, Waters Corporation, USA) on an Ultimate 3000 system

(Thermo Fisher Scientific, USA). A linear gradient from 5% to 45% buffer B (80% acetonitrile in 20 mM ammonium formate, pH 10.0) over 40 minutes was applied, and 12 fractions were collected. The fractions were dried and reconstituted for LC-MS/MS analysis.

For LC-MS/MS, the peptides were further separated on a 25 cm x 75 μm i.d. analytical column (IonOpticks) using a 60-minute gradient. The separation and mass spectrometry analysis were performed using an UltiMate 3000 system coupled with a timsTOF Pro mass spectrometer (Bruker Daltonics, Germany) in both DDA-PASEF and DIA-PASEF modes. The spectral library generated from DDA-PASEF data was used to optimize the DIA-PASEF method, specifically for selecting precursor isolation windows and collision energy settings.

RNA-seq

RNA samples were prepared using the SMART-seq2 protocol and sequenced on an Illumina NovaSeq system. Quality control was performed using the RNA Nano 6000 Assay Kit. Data were processed by Novogene Co., Ltd.

Immunofluorescence staining

Brain sections were immunostained for DAT and ALDH1A1, followed by imaging with an Olympus VS200 slide scanner and a Leica SP8 confocal microscope.

QUANTIFICATION AND STATISTICAL ANALYSIS

The data analysis in this study encompassed multiple steps, including quality control, statistical analysis, functional and pathway enrichment analysis, and network analysis. Spectronaut software was employed to determine protein quality values in the quantitative protein analysis. The transcriptomics data were processed by removing low-quality reads and calculating Q20, Q30, and GC content. Transcriptome data were aligned to the Mus musculus reference genome (GRCm38/mm10) using HISAT2. Quality control assessments involved histograms, boxplots, and principal component analysis (PCA). All quantitative data were filtered by >50%.

For differential protein and transcript analysis, a One-way ANOVA was applied, with an adjusted p-value < 0.05 and a log2 fold change $> |1|$. Tukey Honestly Significant Difference (HSD) post hoc test was then used to identify specific pairwise comparisons exhibiting statistically significant differences. N = 5/3 biological replicates per group were used. The results for each gene, including One-way ANOVA (p-value), Tukey p-value, and Fold Change data, are included in Table S2 for developmental stage comparisons (7vs30, 7vs60, 30vs60), and in Tables S5, S6, and S7 for spatial comparisons (NvsV, NvsS, SvsV).

Pearson correlation analysis was used to assess the relationship between mRNA and protein expression levels. Positively correlated genes were defined as those with a Pearson correlation coefficient (r) ≥ 0.5, and negatively correlated genes were those with r $\leq$ -0.5. The Pearson correlation coefficient was also used to generate the correlation heatmap, which visualizes the strength and direction of linear relationships between samples. Gene Ontology (GO) enrichment analysis and KEGG pathway analysis were conducted using the clusterProfiler R package to identify significant biological processes (BP), molecular functions(MF), cellular components (CC), and pathways. The protein-protein interaction (PPI) network was analyzed using the STRING database and visualized in Cytoscape.

One-way ANOVA and Two-way repeated measures ANOVA were applied to analyze ALDH1A1 protein expression and fluorescence intensity. Detailed statistical information is available in Table S11.